The Plant Cell, Vol. 25: 4101–4109, October 2013, www.plantcell.org

Plant Purine Nucleoside Catabolism Employs a Guanosine Deaminase Required for the Generation of Xanthosine in *Arabidopsis*[W]

Kathleen Dahncke and Claus-Peter Witte[1]

Department of Plant Biochemistry, Dahlem Centre of Plant Sciences, Freie Universität Berlin, 14195 Berlin, Germany

ORCID IDs: 0000-0002-5371-9188 (K.D.); 0000-0002-3617-7807 (C.-P.W.).

Purine nucleotide catabolism is common to most organisms and involves a guanine deaminase to convert guanine to xanthine in animals, invertebrates, and microorganisms. Using metabolomic analysis of mutants, we demonstrate that *Arabidopsis thaliana* uses an alternative catabolic route employing a highly specific guanosine deaminase (GSDA) not reported from any organism so far. The enzyme is ubiquitously expressed and deaminates exclusively guanosine and 2'-deoxyguanosine but no other aminated purines, pyrimidines, or pterines. GSDA belongs to the cytidine/deoxycytidylate deaminase family of proteins together with a deaminase involved in riboflavin biosynthesis, the chloroplastic tRNA adenosine deaminase Arg and a predicted tRNA-specific adenosine deaminase 2 in *A. thaliana*. GSDA is conserved in plants, including the moss *Physcomitrella patens*, but is absent in the algae and outside the plant kingdom. Our data show that xanthosine is exclusively generated through the deamination of guanosine by GSDA in *A. thaliana*, excluding other possible sources like the dephosphorylation of xanthosine monophosphate. Like the nucleoside hydrolases NUCLEOSIDE HYDROLASE1 (NSH1) and NSH2, GSDA is located in the cytosol, indicating that GMP catabolism to xanthine proceeds in a mostly cytosolic pathway via guanosine and xanthosine. Possible implications for the biosynthetic route of purine alkaloids (caffeine and theobromine) and ureides in other plants are discussed.

INTRODUCTION

Purine nucleotides are building blocks of nucleic acids and many cofactors. Most organisms are capable of nucleotide de novo synthesis and nucleobase salvage but also of nucleotide degradation. In plants, the degradation reactions serve to use purine nucleotides as nutrient sources (Stasolla et al., 2003; Zrenner et al., 2006). For this purpose, plants can degrade purine nucleotides completely, oxidizing and hydrolyzing the purine ring to glyoxylate, carbon dioxide, and ammonia (Werner et al., 2010; Werner and Witte, 2011). Also, many microbes fully degrade purine nucleotides, whereas mammals catabolize the purine ring only partially to uric acid or allantoin, which are used to excrete excess nitrogen (Vogels and Van der Drift, 1976). In all organisms investigated to date, xanthine is generated from the purine bases of AMP and GMP, although the enzymes employed and the metabolic pathways used may differ between organismal classes and are still poorly defined in vivo. The degradation of GMP is initiated by its dephosphorylation to guanosine. The Rib moiety of guanosine (and other nucleosides) is removed either by phosphorolysis or hydrolysis, giving rise to (1) guanine (and other nucleobases) and to (2) Rib 1-phosphate or Rib, respectively. *Arabidopsis thaliana* lacks nucleoside phosphorylases but possesses two intracellular nucleoside hydrolases (NUCLEOSIDE HYDROLASE1 [NSH1] and NSH2) with overlapping function in purine and pyrimidine nucleoside catabolism (Jung et al., 2009, 2011; Riegler et al., 2011). However, it has not been shown that these enzymes hydrolyze guanosine. In principle, there are two possible routes of guanosine degradation in plants: It may be (1) deaminated to xanthosine by a guanosine deaminase (GSDA) and then hydrolyzed to xanthine and Rib by NSH1/NSH2 or (2) first hydrolyzed to guanine and then deaminated to xanthine by a guanine deaminase (GDA). GSDA activity has been detected in plant extracts (Katahira and Ashihara, 2006; Deng and Ashihara, 2010), but a gene for such an enzyme has not been cloned from any plant nor any other source so far. By contrast, GDA genes are well known, and the corresponding activity occurs in many organisms (Yuan et al., 1999; Maynes et al., 2000; Nygaard et al., 2000). There are two evolutionary origins for GDA (Nygaard et al., 2000; Fernández et al., 2009). The majority of species, including human and *Escherichia coli*, employ a protein that is member of the amidohydrolase family (Pfam profile PF01979), while a few prokaryotic organisms, including *Bacillus subtilis*, possess a protein belonging to the cytidine/deoxycytidylate deaminase family (Pfam profile PF00383).

Here, we report the genetic identification of a (2'-deoxy-) GSDA of *A. thaliana*. A metabolic analysis of mutants revealed that GSDA is required for guanosine deamination in this plant. Xanthosine is exclusively generated via GSDA, demonstrating that possible alternative sources of xanthosine, such as the dephosphorylation of xanthosine monophosphate (XMP) or the oxidation of inosine, are not relevant in vivo.

RESULTS

Identification of GSDA from *A. thaliana*

Based on the working hypothesis that plants, like many other organismal classes, might possess a GDA, we searched the

[1] Address correspondence to cpwitte@zedat.fu-berlin.de.
The author responsible for distribution of materials integral to the findings presented in this article in accordance with the policy described in the Instructions for Authors (www.plantcell.org) is: Claus-Peter Witte (cpwitte@zedat.fu-berlin.de).
[W] Online version contains Web-only data.
www.plantcell.org/cgi/doi/10.1105/tpc.113.117184

Arabidopsis protein database at The Arabidopsis Information Resource using BLASTP for putative orthologs to GDA from *E. coli* or to the evolutionary unrelated GDA from *B. subtilis*. Proteins with significant similarity to GDA from *E. coli* were not found, whereas five proteins with similarity (U.S. National Center for Biotechnology Information BLAST E-values < 0.001) to GDA from *B. subtilis* were identified. These are encoded by the loci At5g28050, At1g68720, At3g05300, At1g48175, and At4g20960 (in order of decreasing similarity). Some of these could be excluded as GDA candidate loci because they were already functionally characterized: The locus At4g20960 was previously shown to code for a deaminase involved in riboflavin biosynthesis (Fischer et al., 2004), and At1g68720 codes for the chloroplastic tRNA adenosine deaminase Arg (Delannoy et al., 2009; Karcher and Bock, 2009). The locus At1g48175 encodes an uncharacterized protein that is highly conserved in plants. The *A. thaliana* protein has 43% identity (60% similarity) to a human protein with known crystal structure (Protein Data Bank accession number 3DH1), which by sequence and structure resembles tRNA-specific ADENOSINE DEAMINASE2 (ADAT2). In yeast, this enzyme catalyzes the adenosine-to-inosine editing of the anticodon loop of several tRNAs and is essential for survival (Gerber and Keller, 1999). Consistent with this, a mutation in the putative *A. thaliana* ortholog is embryo lethal (http://www.seedgenes.org; profile EMB2191). We concluded that locus At1g48175 likely codes for ADAT2 in *A. thaliana*. Locus At3g05300 is conserved only in a small group of Brassicaceae (sequence information is available for *Arabidopsis lyrata*, *Capsella rubella*, *Brassica rapa*, and *Raphanus raphanistrum*). Whereas in *B. rapa* and *R. raphanistrum* this gene is expressed (based on EST data), there is no evidence for a transcript from At5g05300 in *A. thaliana*. Additionally, the reading frame seems truncated in *A. thaliana* attributable to a base deletion (see Supplemental Figure 1 online). We conclude that At3g05300 likely represents a pseudogene.

The protein encoded at locus At5g28050 possesses the highest overall similarity to GDA from *B. subtilis* (44%). Several residues are conserved that are important for substrate interaction deduced from the crystal structure analysis of the *B. subtilis* enzyme (Liaw et al., 2004; see Supplemental Figure 2 online). A cDNA for this plant GDA candidate was cloned engineering a StrepII-tag coding sequence to the 5′ end. N-terminal tagging was chosen because a Tyr residue at the C terminus of the enzyme may be important for substrate binding (see Supplemental Figure 2 online) and would be masked by a tag. Transient expression in *Nicotiana benthamiana* and affinity purification resulted in highly purified protein for biochemical analyses. The identity of the protein was confirmed by immunoblot using antiserum raised against the candidate protein (see Supplemental Figure 3 online). The activity of the enzyme was assessed using a range of nucleotides, nucleosides, and nucleobases as well as pterines, all possessing amino group substitutions on the respective rings. To our surprise, the enzyme deaminated exclusively guanosine at a high rate (Figure 1A) and showed no or very low activity with all other tested substrates, including guanine. Further enzymatic assays revealed that 2'-deoxyguanosine also is a substrate. We conclude that we identified a (2'-deoxy) GSDA. Kinetic measurements for both substrates were performed (Figures 1B and 1C). Michaelis-Menten constants of 264.0 ± 58.2 μM (confidence interval, P = 95%) and 576.1 ± 217 μM (confidence interval, P = 95%) and turnover numbers of 1.753 s^{-1} and 0.611 s^{-1} were determined for guanosine and 2'-deoxyguanosine, respectively, resulting in catalytic efficiencies of 6642.09 $(s\ M)^{-1}$ and 1061.26 $(s\ M)^{-1}$. A group of 23 compounds was tested as potential inhibitors or activators of the enzyme (see Supplemental Table 1 online) but none had an influence on the activity.

Assessment of GSDA Function in Vivo

To assess if GSDA plays a role in the catabolism of guanosine in vivo, two T-DNA insertion mutants were isolated from the SAIL (Sessions et al., 2002) and GABI-Kat (Kleinboelting et al., 2012) collections (Figure 2A). In homozygous lines of SAIL_305B08 (*gsda*-1) and GK_432D08 (*gsda*-2), *GSDA*-specific transcript

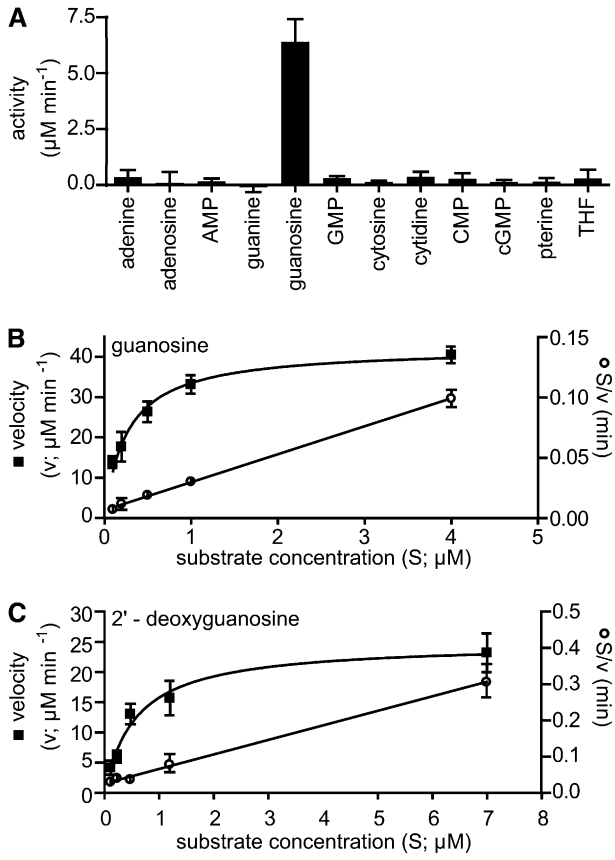

Figure 1. Enzymatic Activity and Determination of Kinetic Constants for GSDA.

(A) Enzymatic activity of GSDA with 1 mM different nucleotides, nucleosides, nucleobases, and pterines as substrates. THF, tetrahydrofolate. Error bars are SD (n = 3).

(B) Left axis, determination of catalytic velocity (v) in terms of ammonia production at different guanosine concentrations fitted using the Michaelis-Menten equation (R^2 = 0.9343). Right axis, Hanes plot: ratio of guanosine concentration and velocity (S/v) plotted against guanosine concentration (S) fitted by linear regression (r^2 = 0.9936). Error bars are SD (n = 5).

(C) As in **(B)** but using 2'-deoxyguanosine as substrate (R^2 = 0.9043, r^2 = 0.9698, n = 4).

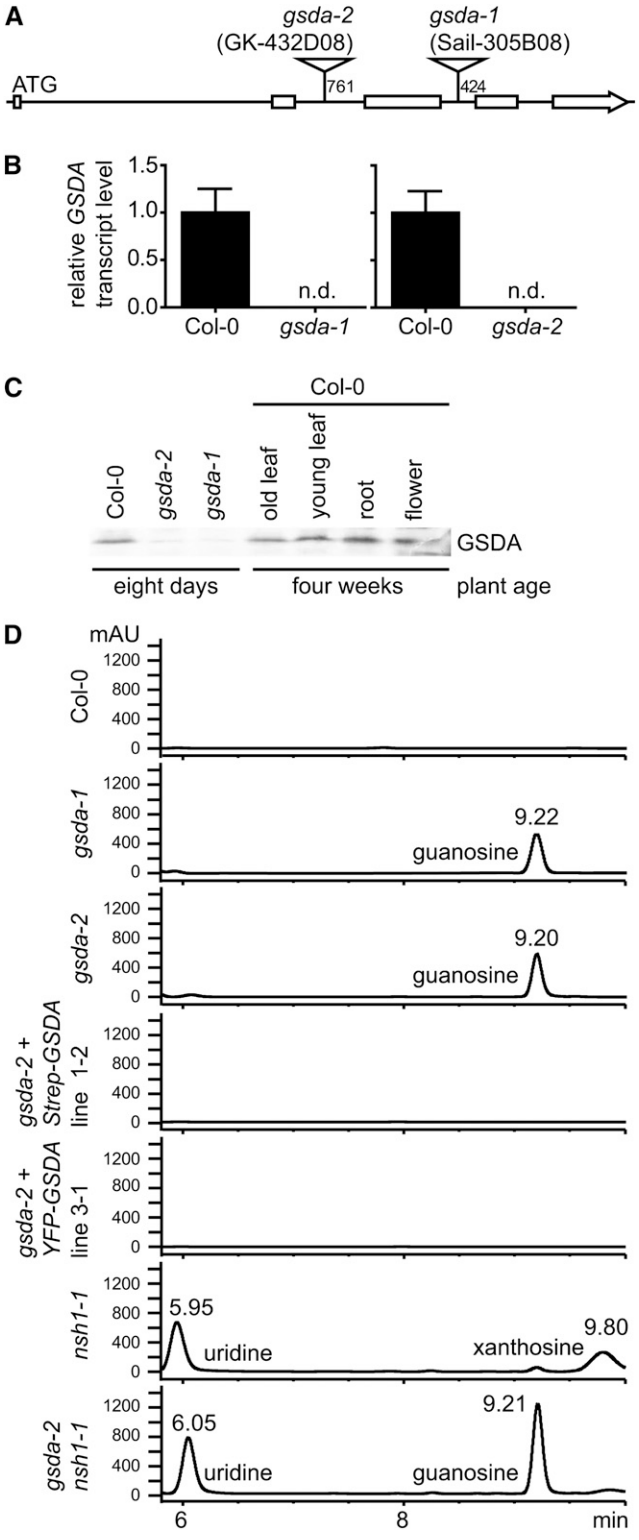

Figure 2. Characterization of Mutants.

(A) The genomic organization of the *GSDA* gene. Boxes represent the exonic regions of the coding sequence. The position of the T-DNA insertions in the respective mutant plant lines are indicated by triangles. Numbers indicate the distance from the first base altered by the insertion to the last base of the stop codon.

(B) Relative quantification of *GSDA* transcript in seedlings of the wild type and the two mutant lines by quantitative PCR using *UBIQUITIN10* as the reference gene. Values have been normalized to mean value of corresponding wild-type samples. Error bars are SD (n = 3; three independent RNA extracts were prepared from a pool of seedlings for each line and used for cDNA synthesis and quantitative PCR). Col-0, Columbia-0; n.d., not detectable.

(C) Assessment of GSDA protein in seedlings of the wild type and the two mutant lines as well as different organs of the wild type by immunoblot employing GSDA-specific antiserum.

(D) Analysis of metabolite extracts using HPLC with photometric detection from dry seeds of the wild type, the two *gsda* mutants, two complementation lines containing either a Strep-tagged or YFP-tagged transgene, the *nsh1-1* mutant, and a double mutant of *gsda-2* and *nsh1-1*. mAU, milliabsorption units.

and GSDA protein were absent (Figures 2B and 2C). Growth and development of both mutants resembled the wild type. In seeds of both mutants, guanosine accumulated, while such accumulation was not observed in the wild type (Figure 2D, first three panels). 2'-Deoxyguanosine was not detected in the mutants, indicating that this compound is of minor significance in vivo. The identity of peaks observed in HPLC traces was confirmed by (1) the retention time of corresponding standards, (2) diode array spectra of compounds, and (3) offline mass spectrometry of compounds collected during HPLC runs (see Supplemental Figure 4 online). The introduction of transgenes resulting in the expression of N-terminally StrepII- or yellow fluorescent protein (YFP)–tagged GSDA into the *gsda-2* mutant background prevented guanosine accumulation in seeds (Figure 2D, panels 4 and 5). The accumulation of guanosine in *gsda* mutants was also observed in leaves, roots, and siliques (Figure 3) and increased with plant age (see Supplemental Figure 5 online). In the wild type, guanosine was not detected in any of the investigated tissues. Together, these data unambiguously link guanosine degradation in vivo to GSDA.

Xanthosine Is Exclusively Generated from Guanosine in Vivo

It was recently reported that mutation of NSH1 (formerly URH1) of *A. thaliana* leads to accumulation of xanthosine and uridine in this plant because the enzyme is required for the hydrolysis of both compounds in vivo (Jung et al., 2011; Riegler et al., 2011). We crossed plants carrying the published *nsh1-1* allele (SALK_083120) with plants possessing the *gsda-2* allele to assess the contribution of GSDA to the xanthosine pool in vivo. As previously reported, the *nsh1* mutant accumulated xanthosine and uridine in seeds but also in leaves and roots (Figures 2D, panel 6, and 3A). In the double mutant, the accumulation of xanthosine was prevented completely, and high guanosine concentrations were observed instead, irrespective of tissue (Figures 2D, panel 7, and 3A). Identical results were obtained when a second unpublished *nsh1* allele (SM_3.39680 from the John Innes Centre SM collection; called *nsh1-2*) was crossed with *gsda-2* mutants and metabolite profiles of seeds were analyzed (see Supplemental Figure 6 online). We conclude that the

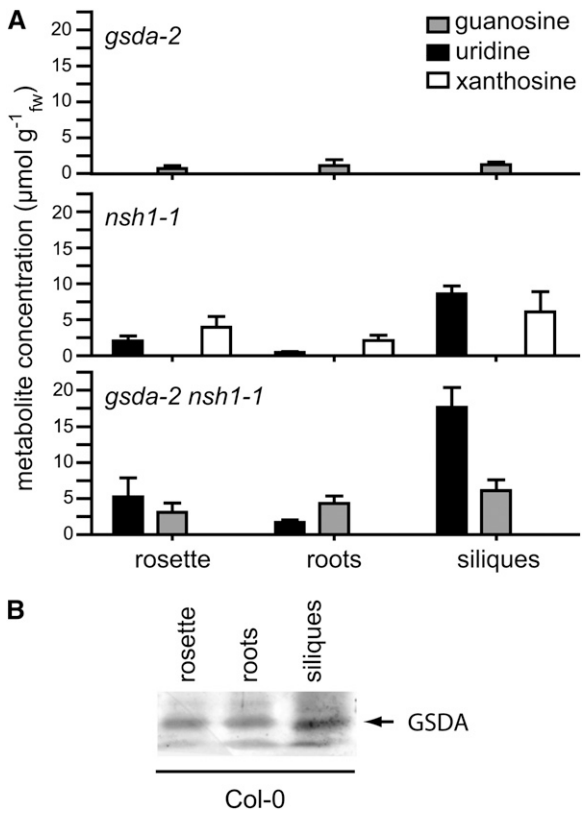

Figure 3. Metabolite Quantification in Different Tissues of Single and Double Mutants.

(A) Concentration of guanosine, xanthosine, and uridine in *gsda-2*, *nsh1-1*, and the *gsda-2 nsh1-1* double mutant in rosette leaves, roots, and yellow siliques of 10-week-old plants grown under long-day conditions. Error bars are SD (n = 5). fw, fresh weight.

(B) Assessment of GSDA protein in corresponding wild-type samples by immunoblot employing GSDA-specific antiserum (8 µg total protein per lane). Col-0, Columbia-0.

only source of xanthosine in vivo is the deamination of guanosine by GSDA. Other possible sources like the dephosphorylation of XMP or the oxidation of inosine do not contribute significantly to the xanthosine pool in vivo. Furthermore, the lack of GSDA in the mutant cannot be compensated for by any other enzyme, although ample guanosine is available as substrate in this genetic background. This demonstrates that the locus At3g05300, which likely represents a pseudogene according to our in silico analysis (see Supplemental Figures 1 and 2 online), can indeed not give rise to a functional GSDA enzyme.

GSDA Is a Cytosolic Enzyme That Is Ubiquitously Expressed

Fusion proteins of GSDA with YFP at the N terminus (YFP-GSDA) located to the cytosol after transient expression in leaves of *N. benthamiana* and in *A. thaliana* protoplasts generated from stable transgenic lines (in *gsda-2* mutant background). The stability of the transgene was demonstrated by immunoblot developed with an anti–green fluorescent protein (GFP) antibody (Figure 4). The tag probably masked any potential N-terminal localization peptide, but unfortunately all of our attempts to express a C-terminally tagged GSDA fusion protein failed. Nonetheless, the location of GSDA is very likely cytosolic because (1) YFP-GSDA is functional in vivo as it prevents the accumulation of guanosine when introduced into the *gsda-2* mutant background (Figure 2D, panel 5), (2) the enzyme was found in the cytosolic fraction in a proteomic study (Ito et al., 2011), (3) most in silico tools predict cytosolic location (SUBA3 database at http://suba.plantenergy.uwa.edu.au), and (4) the downstream enzymes NSH1 and xanthine dehydrogenase are located in the cytosol as well (Jung et al., 2009; Werner and Witte, 2011). Integrating published information and our data, we conclude that the reactions of purine catabolism from guanosine to uric acid via xanthosine and xanthine catalyzed by GSDA, NSH1/NSH2, and xanthine dehydrogenase are located in the cytosol. Uric acid is then imported into the peroxisome for further degradation (Werner and Witte, 2011).

GSDA is ubiquitously expressed in *A. thaliana* because the protein is detected in all investigated tissues and guanosine accumulates in the respective tissues in the *gsda* mutant (Figure 3). Additionally, plant lines carrying a transgene with a 1000-bp genomic fragment upstream of the *GSDA* start codon fused to β-glucuronidase (GUS) showed ubiquitous blue staining (see Supplemental Figure 7 online). GSDA transcript is well detected in all tissues and cell types according to microarray data (for

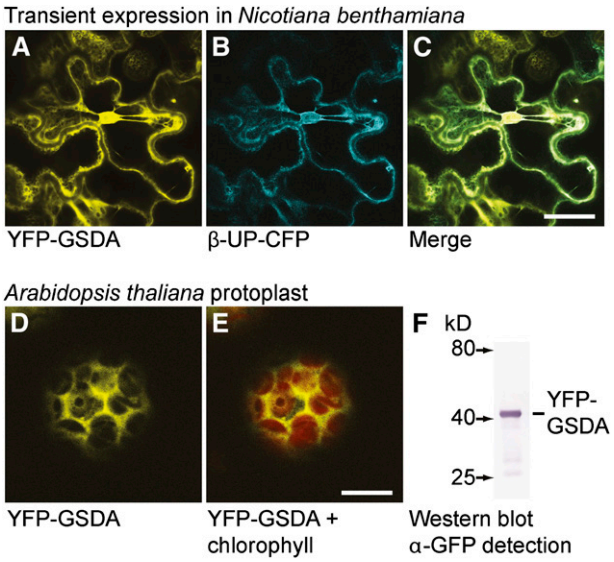

Figure 4. Subcellular Localization of GSDA.

(A) to **(C)** Confocal fluorescence microscopy images of lower leaf epidermis cells of *N. benthamiana* transiently expressing N-terminally YFP-tagged GSDA (YFP-GSDA) and C-terminally CFP-tagged cytosolic protein (β-UP-CFP). YFP **(A)**, CFP **(B)**, and YFP + CFP **(C)** fluorescence, respectively. Bar = 20 µm.

(D) and **(E)** Mesophyll cell protoplast of lines carrying a *YFP-GSDA* transgene. YFP fluorescence **(D)** and YFP + chlorophyll autofluorescence **(E)**. Bar = 10 µm.

(F) Stability of the YFP-GSDA fusion protein after transient expression in *N. benthamiana* analyzed by immunoblot developed with a GFP-specific antibody.

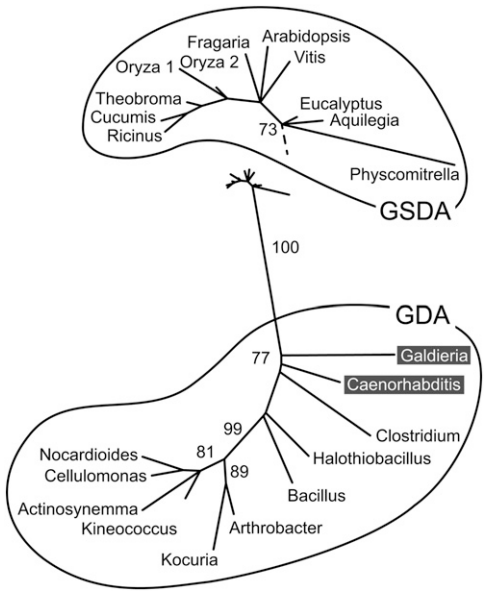

Figure 5. Phylogenetic Analysis of the GDA/GSDA Protein Subfamily.

The sequence alignment of Supplemental Figure 8 online (available as Supplemental Data Set 1 online) was used to construct a phylogenetic tree employing the MEGA5 software (maximum likelihood, WAG+G model, nearest neighbor interchange). A consensus tree from 1000 bootstraps was constructed. Only bootstrap values above 70 are shown. The GSDA portion of the tree was amplified 5 times to better visualize the branching pattern. Eukaryotes within the GDA portion of the tree are indicated by dark background.

example, see the eFP browser at http://bar.utoronto.ca/efp/cgi-bin/efpWeb.cgi). We conclude that GSDA is ubiquitously expressed in *A. thaliana* consistent with its role in a primary metabolic pathway.

GSDA Is Unique to Plants

Orthologs to GSDA are found in each plant genome sequenced to date, mostly in single copy, but not in the green algae. Similarities between plant sequences are high even in taxonomically distant species (see Supplemental Figure 8 online), for example, 94.1% between GSDA from *A. thaliana* and the ortholog from rice encoded at the locus Os03g61810. A sequence comparison of plant GSDAs with bacterial GDAs reveals that residues required for deamination in the cytidine/deoxycytidylate deaminase superfamily are conserved in both groups and that all residues required for substrate binding deduced from the crystal structure of GDA of *B. subtilis* (Liaw et al., 2004) are conserved between GSDAs and GDAs, with the notable exception of a Trp at position 92 in GDA, which is exchanged for Leu in plant GSDAs (see Supplemental Figure 8 online). These sequence hallmarks make it easy to discern GSDA from other similar proteins of the cytidine/deoxycytidylate deaminase family encoded in plant genomes (see Supplemental Figure 2 online). The location of Trp-92 in the active site of GDA from *B. subtilis* precludes the binding of guanosine by clashing with the Rib moiety (Liaw et al., 2004). We speculated that the presence of Leu instead of Trp in GSDA might allow the binding of guanosine in the active site. This hypothesis was tested by exchanging Leu-119 of GSDA from *A. thaliana* for Trp or by altering the whole HLS motif (residues 118 to 120) to YWA found in the *B. subtilis* GDA enzyme. The variant enzymes lost enzymatic activity with guanosine but also did not display any activity with guanine. The reverse exchanges in GDA of *B. subtilis* (Trp-92 to Leu or YWA motif to HLS) also abolished all enzymatic activity (see Supplemental Figure 9 online). We conclude that Leu-119 and Trp-92 have functional relevance for GSDA and GDA, respectively, but their exchange alone or within their respective sequence contexts is not sufficient to change substrate specificity of these enzymes. Nonetheless, when Trp (at an equivalent position to Trp-92) is present in a GDA/GSDA subfamily protein, then the respective enzyme will likely catalyze guanine and not guanosine deamination. Based on this assumption, GSDA does not occur outside the plant kingdom because Trp-92 is highly conserved in nonplant GDA/GSDA subfamily proteins. This includes proteins of eukaryotic origin from nematodes (for example *Caenorhabditis elegans*) and red algae (for example *Galdieria sulphuraria*; see Supplemental Figure 8 online), which contain Trp-92 and are overall more similar to GDA than GSDA. These conclusions are backed up by a phylogenetic analysis clearly separating the GDA and GSDA subfamilies and assigning the *C. elegans* and *G. sulphuraria* sequences to the GDA group (Figure 5). Up to now, GDA of the cytidine/deoxycytidylate deaminase type has been documented only in prokaryotes (Fernández et al., 2009).

DISCUSSION

There have been sporadic reports about GSDA activity in mammals, but Roberts (2003) demonstrated that in human serum and tissue extracts guanosine deamination is catalyzed by the combined action of nucleoside phosphorylase and GDA. In prokaryotes, a GSDA has been partially purified and characterized from only one organism (*Pseudomonas putida*; Ishida et al., 1969), but the genetic origin of this potential GSDA and its relevance for guanosine deamination in vivo remain unknown. In plants, GSDA

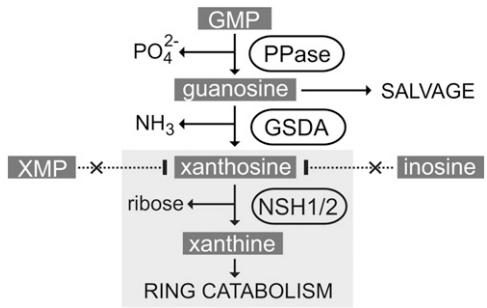

Figure 6. Model of the Metabolic Pathway for GMP Degradation in *A. thaliana*.

GMP is dephosphorylated by a so far unknown phosphatase (PPase) to guanosine, which is either deaminated to xanthosine by GSDA or salvaged into nucleotides and nucleic acids. The hydrolysis of xanthosine to xanthine and Rib is catalyzed by NSH1 possibly with the participation of NSH2. In general, xanthosine and xanthine cannot be salvaged and are destined for degradation via purine ring catabolism (gray shaded area). Neither XMP nor inosine gives rise to xanthosine in vivo.

activity has been detected in cell-free extracts of potato (*Solanum tuberosum*) tubers (Katahira and Ashihara, 2006), and the enzyme has been partially purified from leaves of tea (*Camellia sinensis*; Negishi et al., 1994). Because GDA activity is generally absent or low in plant extracts (Katahira and Ashihara, 2006), it has been proposed that GSDA is the main deaminating activity in the catabolic route from GMP to xanthine (Stasolla et al., 2003). Our data corroborate this view, leading us to outline the in vivo route of GMP degradation as shown in Figure 6. GMP is first dephosphorylated by an unknown phosphatase. The resulting guanosine is then deaminated to xanthosine in the cytosol by GSDA followed by xanthosine hydrolysis to xanthine and Rib employing the cytosolic NSH1 enzyme.

The direct involvement of NSH2 in this last reaction is still uncertain. Isolated NSH2 has not yet been characterized biochemically, but extracts of an *nsh2* mutant line show strongly reduced xanthosine hydrolase activity (Riegler et al., 2011). However, the *nsh2* mutant does not accumulate xanthosine as observed in the *nsh1* mutant (Jung et al., 2011; Riegler et al., 2011). In *A. thaliana*, xanthosine is exclusively generated by guanosine deamination, which demonstrates that other sources of xanthosine like the dephosphorylation of XMP or the oxidation of inosine are not relevant in vivo. This is not surprising for the latter reaction because no inosine dehydrogenase has been identified in any species. However, XMP dephosphorylation has been postulated to occur when inosine monophosphate (IMP) is degraded to form ureides in nodules of ureide-exporting legumes (Shelp and Atkins, 1983) and for the generation of purine alkaloids (caffeine and theobromine) from IMP in coffee (*Coffea arabica*) and tea (Ito and Ashihara, 1999; Koshiishi et al., 2001; Keya et al., 2003), although direct evidence for XMP dephosphorylation in vivo is lacking. Nonetheless, all current reviews of plant nucleotide metabolism also include an XMP-to-xanthosine dephosphorylation reaction in their overview schemes (Stasolla et al., 2003; Zrenner et al., 2006; Ashihara et al., 2008). Although this reaction might occur in plants other than *A. thaliana*, it is also possible that IMP conversion to ureides or to purine alkaloids actually occurs via XMP to GMP and then guanosine to give rise to xanthosine catalyzed by GSDA. This option is consistent with the currently available data and has not been tested so far. In this case, GSDA would exert a key function, possibly regulating the flux of IMP into (1) purine alkaloids in plants that produce these compounds, (2) ureides in the nodules of ureide producing legumes, and (3) purine degradation from GMP in all plants.

That GSDA is positioned at a crossroad of metabolism is indicated by the observation that labeled guanosine applied to plants or isolated plant tissues can either be salvaged into nucleotides and nucleic acids or degraded (Ashihara et al., 1997; Deng and Ashihara, 2010). By contrast, xanthosine is exclusively degraded and cannot be salvaged (Figure 6; Koyama et al., 2003; Katahira and Ashihara, 2006; Ashihara, 2012). Once deaminated by GSDA, the fate of the nucleoside is decided. If there is regulation of GSDA activity, it might have an allosteric component. However, none of 23 compounds we tested influenced GSDA activity (see Supplemental Table 1 online). The unaltered growth of the *gsda* mutants indicates that the lack of guanosine catabolism does not strongly affect plant growth and development when plants are kept under standard laboratory and greenhouse conditions. Consistent with this, other mutants of purine nucleoside or purine ring catabolic genes do not show phenotypes under such conditions (Riegler et al., 2011; Werner et al., 2013), but some are affected when exposed to several days of darkness (Brychkova et al., 2008; Jung et al., 2011).

Why does guanosine accumulate in *gsda* mutants if this compound can be salvaged? The steady state level of guanosine may need to increase until the flux into the salvage reaction (s) balances GMP dephosphorylation. If the subcellular sites of guanosine generation and salvage are different, the adjustment of a new equilibrium may also include diffusion and transport processes. In topinambour (*Helianthus tuberosus*), for example, inosine guanosine kinase activity is located in the mitochondria (Combes et al., 1989). The accumulation of guanosine also indicates that guanosine hydrolysis to guanine is not a predominant reaction in vivo. In accordance, recombinant NSH1 produced in *E. coli* did not have guanosine hydrolase activity in our hands (data not shown). Taken together with the general absence of GDA activity in plant extracts (Stasolla et al., 2003) and the absence of an orthologous gene encoding known types of GDA in plant genomes, the existence of an alternative route of guanosine to xanthine conversion via guanine appears unlikely.

In summary, our data show that plants use a different pathway for GMP catabolism than do other species. It will be interesting to investigate if GSDA plays a key role in regulating the flux into the purine ring catabolic pathway, possibly also for AMP, and to elucidate the function of GSDA for ureide generation in legumes and for purine alkaloid generation in plants like coffee and tea.

METHODS

Plant Material and Growth Conditions

T-DNA mutants of *Arabidopsis thaliana* from the SALK collection (SALK_083120, *nsh1-1*; Alonso et al., 2003) and the SAIL collection (SAIL305B08, *gsda-2*; Sessions et al., 2002) as well as an En/Spm transposon line (SM3-39680, *nsh1-2*) from the John Innes Centre SM collection (Tissier et al., 1999) were ordered from the European Arabidopsis Stock Centre. A GABI-Kat T-DNA mutant (GK432D08, *gsda-1*; Kleinboelting et al., 2012) was received from the GABI-Kat mutant collection at the Max-Planck-Institute for Plant Breeding Research. Plants were cultivated as described by Witte et al. (2005) for the isolation of homozygous mutants (employing primers listed in Supplemental Table 2 online) and for metabolite analyses. Double mutants were obtained by crossing *gsda-2* and *nsh1-1* as well as *nsh1-2* and *gsda-2* mutants (pollen donor named last, respectively). To isolate mesophyll protoplasts, plants were grown on Jiffy7 soil in a controlled growth chamber with a short photoperiod (8 h light, 20°C day, 18°C night, and 60% relative humidity). *Nicotiana benthamiana* was grown and transgenic *A. thaliana* generated as described by Witte et al. (2004). Transient expression in *N. benthamiana* was performed as described by Werner et al. (2008). For confocal microscopy, YFP-AtGSDA and β-UP-CFP (for β-ureidopropionase–cyan fluorescent protein) were coexpressed by mixing the respective transgenic *Agrobacterium tumefaciens* strains and agrobacteria expressing the p19 silencing inhibitor from tomato bushy stunt virus.

Real-Time PCR Analysis of Mutants

To determine the gene-specific transcript level in the *gsda* mutants in comparison to the wild type, seedlings of the corresponding lines were harvested and pooled. RNA was prepared using TRIsure reagent (Bioline) and treated with RNase-free DNase (Fermentas) following the manufacturers'

instructions. The reverse transcription was performed using 600 ng of total RNA and the SuperscriptIII SuperMix (Invitrogen) according to the manufacturer's protocol.

In a final volume of 10 μL, quantitative real-time PCR analysis was performed referring to the instructions of Power SYBR Green PCR Master Mix (Applied Biosystems) using the CFX96 system (Bio-Rad). Specificity of the amplification reactions was assessed using postamplification dissociation curves. *UBIQUITIN10* was used as reference gene for quantification of gene expression and amplified using primers 2535 + 2536. Primers N0342 + N0343 were used for *gsda-2* and N0346 + N0347 for *gsda-1*. Both pairs are flanking the corresponding insertion.

Cloning and Site-Directed Mutagenesis

For cloning of the *GSDA* coding sequence, cDNA from seedlings was prepared as described above. *GSDA* was amplified by PCR using primers 1899 and 1900, introducing an *Nco*I and a *Bam*HI site and cloned into pXNS2pat-Strep (Cao et al., 2010) and pET30a (Novagen). The latter plasmid served for expression of GSDA in *Escherichia coli* to produce protein for antibody production. To generate a binary vector that allows for the expression of fusion proteins containing an N-terminal YFP tag, *eYFP* was amplified from pXCS-YFP (Feys et al., 2005) using primers 2209 + 2210, introducing a *Sac*I and *Sfo*I site. The fragment replaced the StrepII-tag in pXNS2pat-Strep, resulting in the new vector pXNS2pat-YFP (accession number KF499077). *GSDA* was cloned into this vector via *Nco*I and *Bam*HI. For colocalization, the cDNA of cytosolic β-UP (At5g64370) was amplified using primers 1237 + 1239, introducing an *Xma*I and an *Eco*RI site and cloned into pXCS-CFP (Feys et al., 2005).

From genomic DNA of *A. thaliana* (Col-0), a fragment of 1147 bp upstream of the GSDA start codon (putative promoter) was amplified using primers 2211 + 2212, introducing an *Asc*I and an *Mfe*I site. The product was inserted into pI2-pCPK28-GUS-mcs2 (Matschi et al., 2013), releasing the promoter of CPK28 (pCPK28) and generating the construct pI2-pGSDA-GUS-mcs2.

GDA from *Bacillus subtilis* was amplified from DNA using primers 2175 + 2176, introducing an *Nde*I and a *Bam*HI site and cloned into pXNS1pat-Strep (Cao et al., 2010).

Site-directed mutagenesis of GSDA was performed with primers (1) N0133 + N1034 and (2) N0135 + N0136 using GSDA in pXNS2pat-Strep as template. For GDA from *B. subtilis*, primers (3) N0138 + N0139 and (4) N0140 + N0141 were used for PCR with GDA in pXNS1pat-Strep as template. PCRs were performed following the QuikChange site-directed mutagenesis protocol (Stratagene).

Protein Purification and Enzymatic Activity Measurements

StrepII-GSDA was affinity purified after transient expression in *N. benthamiana* as described by Werner et al. (2008). To determine the substrate specificity of GSDA, different potential substrates (see Supplemental Table 1 online) were used. All substrates were prepared as 2 mM solution in wash buffer (100 mM HEPES, pH 8.0, 100 mM NaCl, 0.5 mM EDTA, and 0.005% Triton X-100). For each reaction, 25 μL of the respective substrate solution and 10 μL of wash buffer were mixed and preincubated at 40°C. The reaction was started after 3 min by the addition of 15 μL of enzyme solution. In a time course, samples of 10 μL were taken and added to 90 μL of water, followed by 25 μL of phenol nitroprusside reagent and 50 μL of hypochlorite reagent for colorimetric ammonia quantification (Witte and Medina-Escobar, 2001). Ammonium standard curves were prepared by adding elution buffer instead of enzyme solution and then diluting in NH_4Cl solutions of different concentrations instead of water prior to detection.

The kinetic constants were determined at final concentrations of 0.1, 0.2, 0.5, 1.0, and 4.0 mM of guanosine (five repeated measurements) or of 0.12, 0.24, 0.48, 1.2, and 7.0 mM of 2'-deoxyguanosine (four repeated measurements). To screen for potential effectors 20 μL of guanosine solution (0.75 mM in wash buffer) was mixed with 15 μL of the respective effector solution (1 mM in wash buffer; see Supplemental Table 1 online) and the reaction started with 15 μL of protein solution as described above. For the analysis of the GSDA activity in comparison to GDA from *B. subtilis* and mutagenized versions of both proteins, 25 μL of a guanosine or guanine solution (2 mM in wash buffer) were preincubated for 3 min at 40°C and the reaction started by addition of 25 μL of the corresponding enzyme solution. Sampling and detection were performed in a time course as described above. Purified protein was quantified using the Nano-Orange kit from Invitrogen as described by Werner et al. (2008).

Metabolite Analyses

Roots, leaves, and siliques were ground in liquid nitrogen using a mortar. Frozen aliquots of 100 mg were passed into 1.5-mL microcentrifuge tubes, and 300 μL of cold 0.5 M $HClO_4$ was added followed by grinding with a rotating pestle. Samples were incubated on ice for 10 min and centrifuged (10 min, 20,000*g*, 4°C) and the supernatant mixed with 15 μL of alkaline potassium carbonate solution (5 M KOH and 2 M K_2CO_3) to precipitate the perchlorate. After incubation for 5 min on ice, samples were centrifuged (15 min, 20,000*g*, 4°C), and supernatants were frozen in liquid nitrogen, thawed, centrifuged again as before, and new supernatants transferred to HPLC sample vials. Seed extraction was performed by grinding 5 mg of material in 100 μL of $HClO_4$with a rotating pestle. The supernatant was removed and the extraction repeated. Both supernatants were incubated on ice for 10 min and centrifuged (15 min, 20,000*g*, 4°C) before they were pooled and mixed with 10 μL of alkaline potassium carbonate solution. All subsequent steps were performed as described above. Standards were treated identically to samples to account for losses and interferences. HPLC analyses were performed using an Agilent 1200 SL system equipped with a diode array detector using an ion pairing reversed phase chromatography method. Samples (20-μL injection volume) were separated on a Polaris 5 C18 A 150 × 4.6-mm column at 25°C using a flow rate of 0.64 mL min^{-1} according to application note 5991-2058EN from Agilent, with several modifications. Mobile phase A consisted of 10 mM tetrabutylammonium hydroxide and 10 mM ammonium acetate, pH 6.5, to make it compatible with mass spectrometry analyses. Mobile phase B consisted of 10 mM tetrabutylammonium hydroxide in methanol. The elution started with 4% mobile phase B. At the break points 2.5, 4, 6, 7, 12, 15, 20, 20.1, and 24 min, the percentage of B was 4, 10, 10, 20, 40, 100, 100, 4, and 4, respectively. Quantification was performed using Agilent Chemstation employing standard solutions of guanosine, xanthosine, and uridine of 50, 100, 200, and 400 μM. For offline mass spectrometry analysis, the substances were collected in a peak-based manner (defined by threshold and slope). Mass spectrometry analysis was performed on an Agilent 6210 electrospray ionization time-of-flight mass spectrometer using a flow rate of 4 μL min^{-1} and an electrospray voltage of 4 kV. The desolvation gas was set to 15 p.s.i. (1 bar). All other parameters were optimized for maximum abundance of each $[M+H]^+$.

Electrophoresis and Immunoblotting

SDS gel electrophoresis, immunoblotting for the detection of StrepII-tagged proteins, as well as Coomassie Brilliant Blue and silver staining were performed according to Witte et al. (2004). YFP-GSDA was detected using an anti-GFP antibody (Roche; dilution 1:1000) and a goat anti-mouse IgG alkaline phosphatase conjugate (Sigma-Aldrich; dilution 1:30,000). GSDA was detected with the generated polyclonal rabbit anti-GSDA antiserum (see Supplemental Methods 1 online; diluted 1:2500 for purified protein; diluted 1:500 for detection in plant extracts) and a mouse anti-rabbit IgG alkaline phosphatase conjugate (Sigma-Aldrich; dilution 1:10,000).

Protoplasting, Subcellular Localization, and GUS Staining

A. thaliana protoplasts were obtained according to Wu et al. (2009). For subcellular localization, mesophyll protoplasts from *A. thaliana* expressing

YFP-GSDA as well as *N. benthamiana* leaves transiently coexpressing YFP-GSDA and β-UP-CFP were analyzed using a Leica True Confocal Scanner SP5 microscope equipped with an HCX PL APO 63.0x1.20 UV water immersion objective. YFP, chlorophyll autofluorescence, and CFP were detected using 514-, 488-, and 458-nm excitation wavelengths and 520- to 550-, 710- to 800-, and 465- to 495-nm emission wavelengths, respectively. Acquired images were processed using the Leica Microsystems Leica Application Suite Advanced Fluorescence software and Adobe Photoshop CS6. Staining for GUS activity was performed according to Matschi et al. (2013).

Data Analysis

Statistical analyses and the determination of kinetic constants were performed with the GraphPad Prism software package.

Accession Numbers

Sequence data from this article can be found in the GenBank/EMBL data libraries under the following accession numbers: At5g28050, GSDA; At1g05620, NSH1; At2g36310, NSH2; At4g34890, xanthine dehydrogenase; At1g68720, chloroplastic A-to-I tRNA editing enzyme; At3g05300, GSDA pseudogene; At1g48175, putative tRNA-specific adenosine deaminase 2; At4g20960, 2,5-diamino-6-ribosylamino-4(3H)-pyrimidinone 5-phosphate deaminase; At5g64370, β-UP; must be: GDA from *E. coli*, Uniprot accession P76641; and must be: GDA from *B. subtilis*, Uniprot accession O34598. Sequence data for the described vector pXNS2pat-YFP can be found in the GenBank/EMBL data libraries under accession number KF499077.

Supplemental Data

The following materials are available in the online version of this article.

Supplemental Figure 1. Comparison of the Genomic Sequence at Locus At3g05300 of *A. thaliana* to the Corresponding Region in the *Brassica napus* Genome.

Supplemental Figure 2. Multiple Sequence Alignment of Guanine Deaminase from *B. subtilis* with Putative Orthologs from *A. thaliana*.

Supplemental Figure 3. Documentation of Strep-GSDA Affinity Purification after Transient Expression in *N. benthamiana*.

Supplemental Figure 4. Offline ESI-MS-MS Analysis of Guanosine, Xanthosine, and Uridine Peaks.

Supplemental Figure 5. Guanosine Accumulation during Development.

Supplemental Figure 6. Seed Metabolite Analysis of Mutants.

Supplemental Figure 7. Promoter GUS Activity Analysis.

Supplemental Figure 8. Multiple Sequence Alignment of GSDA and GDA Protein Sequences.

Supplemental Figure 9. Analysis of GSDA and GDA Active Site Mutants.

Supplemental Table 1. Compounds Tested as Substrates or as Potential Effectors.

Supplemental Table 2. Primers Used in This Study.

Supplemental Methods 1. Generation of Antiserum against GSDA.

Supplemental Data Set 1. Multiple Protein Alignment Shown in Supplemental Figure 8 in Phylip 3.0 Format.

ACKNOWLEDGMENTS

This research was funded by the Deutsche Forschungsgemeinschaft (Grant DFG WI3411/1-2) and the German Academic Exchange Service from funds of the German Federal Ministry for Education and Research, program German-Chinese Research Groups.

AUTHOR CONTRIBUTIONS

K.D. planned and conducted all experiments. C.-P.W. was responsible for the experimental outline, bioinformatic analyses, and writing the article.

Received August 7, 2013; revised September 19, 2013; accepted September 27, 2013; published October 15, 2013.

REFERENCES

Alonso, J.M., et al. (2003). Genome-wide insertional mutagenesis of *Arabidopsis thaliana*. Science **301:** 653–657.

Ashihara, H. (2012). Xanthosine metabolism in plants: Metabolic fate of exogenously supplied C-14-labelled xanthosine and xanthine in intact mungbean seedlings. Phytochem. Lett. **5:** 100–103.

Ashihara, H., Sano, H., and Crozier, A. (2008). Caffeine and related purine alkaloids: Biosynthesis, catabolism, function and genetic engineering. Phytochemistry **69:** 841–856.

Ashihara, H., Takasawa, Y., and Suzuki, T. (1997). Metabolic fate of guanosine in higher plants. Physiol. Plant. **100:** 909–916.

Brychkova, G., Alikulov, Z., Fluhr, R., and Sagi, M. (2008). A critical role for ureides in dark and senescence-induced purine remobilization is unmasked in the Atxdh1 *Arabidopsis* mutant. Plant J. **54:** 496–509.

Cao, F.Q., Werner, A.K., Dahncke, K., Romeis, T., Liu, L.H., and Witte, C.P. (2010). Identification and characterization of proteins involved in rice urea and arginine catabolism. Plant Physiol. **154:** 98–108.

Combes, A., Lafleuriel, J., and Lefloch, F. (1989). The inosine-guanosine kinase-activity of mitochondria in tubers of Jerusalem Artichoke. Plant Physiol. Biochem. **27:** 729–736.

Delannoy, E., Le Ret, M., Faivre-Nitschke, E., Estavillo, G.M., Bergdoll, M., Taylor, N.L., Pogson, B.J., Small, I., Imbault, P., and Gualberto, J.M. (2009). *Arabidopsis* tRNA adenosine deaminase arginine edits the wobble nucleotide of chloroplast tRNAArg(ACG) and is essential for efficient chloroplast translation. Plant Cell **21:** 2058–2071.

Deng, W.W., and Ashihara, H. (2010). Profiles of purine metabolism in leaves and roots of *Camellia sinensis* seedlings. Plant Cell Physiol. **51:** 2105–2118.

Fernández, J.R., Byrne, B., and Firestein, B.L. (2009). Phylogenetic analysis and molecular evolution of guanine deaminases: From guanine to dendrites. J. Mol. Evol. **68:** 227–235.

Feys, B.J., Wiermer, M., Bhat, R.A., Moisan, L.J., Medina-Escobar, N., Neu, C., Cabral, A., and Parker, J.E. (2005). *Arabidopsis* SENESCENCE-ASSOCIATED GENE101 stabilizes and signals within an ENHANCED DISEASE SUSCEPTIBILITY1 complex in plant innate immunity. Plant Cell **17:** 2601–2613.

Fischer, M., Römisch, W., Saller, S., Illarionov, B., Richter, G., Rohdich, F., Eisenreich, W., and Bacher, A. (2004). Evolution of vitamin B2 biosynthesis: Structural and functional similarity between pyrimidine deaminases of eubacterial and plant origin. J. Biol. Chem. **279:** 36299–36308.

Gerber, A.P., and Keller, W. (1999). An adenosine deaminase that generates inosine at the wobble position of tRNAs. Science **286:** 1146–1149.

Ishida, Y., Shirafuj, H., Kida, M., and Yoneda, M. (1969). Studies on guanosine degrading system in bacterial cell. 3. Purification and properties of guanosine deaminase. Agric. Biol. Chem. **33:** 384–390.

Ito, E., and Ashihara, H. (1999). Contribution of purine nucleotide biosynthesis de novo to the formation of caffeine in young tea (*Camellia sinensis*) leaves. J. Plant Physiol. **154:** 145–151.

Ito, J., Batth, T.S., Petzold, C.J., Redding-Johanson, A.M., Mukhopadhyay, A., Verboom, R., Meyer, E.H., Millar, A.H., and Heazlewood, J.L. (2011). Analysis of the *Arabidopsis* cytosolic proteome highlights subcellular partitioning of central plant metabolism. J. Proteome Res. **10:** 1571–1582.

Jung, B., Flörchinger, M., Kunz, H.H., Traub, M., Wartenberg, R., Jeblick, W., Neuhaus, H.E., and Möhlmann, T. (2009). Uridine-ribohydrolase is a key regulator in the uridine degradation pathway of *Arabidopsis*. Plant Cell **21:** 876–891.

Jung, B., Hoffmann, C., and Möhlmann, T. (2011). *Arabidopsis* nucleoside hydrolases involved in intracellular and extracellular degradation of purines. Plant J. **65:** 703–711.

Karcher, D., and Bock, R. (2009). Identification of the chloroplast adenosine-to-inosine tRNA editing enzyme. RNA **15:** 1251–1257.

Katahira, R., and Ashihara, H. (2006). Profiles of purine biosynthesis, salvage and degradation in disks of potato (*Solanum tuberosum* L.) tubers. Planta **225:** 115–126.

Keya, C.A., Crozier, A., and Ashihara, H. (2003). Inhibition of caffeine biosynthesis in tea (*Camellia sinensis*) and coffee (*Coffea arabica*) plants by ribavirin. FEBS Lett. **554:** 473–477.

Kleinboelting, N., Huep, G., Kloetgen, A., Viehoever, P., and Weisshaar, B. (2012). GABI-Kat SimpleSearch: New features of the *Arabidopsis thaliana* T-DNA mutant database. Nucleic Acids Res. **40** (Database issue)**:** D1211–D1215.

Koshiishi, C., Kato, A., Yama, S., Crozier, A., and Ashihara, H. (2001). A new caffeine biosynthetic pathway in tea leaves: Utilisation of adenosine released from the S-adenosyl-L-methionine cycle. FEBS Lett. **499:** 50–54.

Koyama, Y., Tomoda, Y., Kato, M., and Ashihara, H. (2003). Metabolism of purine bases, nucleosides and alkaloids in theobromine-forming *Theobroma cacao* leaves. Plant Physiol. Biochem. **41:** 977–984.

Liaw, S.H., Chang, Y.J., Lai, C.T., Chang, H.C., and Chang, G.G. (2004). Crystal structure of *Bacillus subtilis* guanine deaminase: The first domain-swapped structure in the cytidine deaminase superfamily. J. Biol. Chem. **279:** 35479–35485.

Matschi, S., Werner, S., Schulze, W.X., Legen, J., Hilger, H.H., and Romeis, T. (2013). Function of calcium-dependent protein kinase CPK28 of *Arabidopsis thaliana* in plant stem elongation and vascular development. Plant J. **73:** 883–896.

Maynes, J.T., Yuan, R.G., and Snyder, F.F. (2000). Identification, expression, and characterization of *Escherichia coli* guanine deaminase. J. Bacteriol. **182:** 4658–4660.

Negishi, O., Ozawa, T., and Imagawa, H. (1994). Guanosine deaminase and guanine deaminase from tea leaves. Biosci. Biotechnol. Biochem. **58:** 1277–1281.

Nygaard, P., Bested, S.M., Andersen, K.A.K., and Saxild, H.H. (2000). *Bacillus subtilis* guanine deaminase is encoded by the yknA gene and is induced during growth with purines as the nitrogen source. Microbiology **146:** 3061–3069.

Riegler, H., Geserick, C., and Zrenner, R. (2011). *Arabidopsis thaliana* nucleosidase mutants provide new insights into nucleoside degradation. New Phytol. **191:** 349–359.

Roberts, E.L.L. (2003). Guanosine deaminase in human serum and tissue extracts—A reappraisal of the products. Br. J. Biomed. Sci. **60:** 197–203.

Sessions, A., et al. (2002). A high-throughput *Arabidopsis* reverse genetics system. Plant Cell **14:** 2985–2994.

Shelp, B.J., and Atkins, C.A. (1983). Role of inosine monophosphate oxidoreductase in the formation of ureides in nitrogen-fixing nodules of cowpea (*Vigna unguiculata* L. Walp.). Plant Physiol. **72:** 1029–1034.

Stasolla, C., Katahira, R., Thorpe, T.A., and Ashihara, H. (2003). Purine and pyrimidine nucleotide metabolism in higher plants. J. Plant Physiol. **160:** 1271–1295.

Tissier, A.F., Marillonnet, S., Klimyuk, V., Patel, K., Torres, M.A., Murphy, G., and Jones, J.D.G. (1999). Multiple independent defective suppressor-mutator transposon insertions in *Arabidopsis*: A tool for functional genomics. Plant Cell **11:** 1841–1852.

Vogels, G.D., and Van der Drift, C. (1976). Degradation of purines and pyrimidines by microorganisms. Bacteriol. Rev. **40:** 403–468.

Werner, A.K., Medina-Escobar, N., Zulawski, M., Sparkes, I.A., Cao, F.Q., and Witte, C.P. (2013). The ureide degrading reactions of purine ring catabolism employ one aminohydrolase and three amidohydrolases in Arabidopsis, soybean and rice. Plant Physiol. **163:** 672–681.

Werner, A.K., Romeis, T., and Witte, C.P. (2010). Ureide catabolism in *Arabidopsis thaliana* and *Escherichia coli*. Nat. Chem. Biol. **6:** 19–21.

Werner, A.K., Sparkes, I.A., Romeis, T., and Witte, C.P. (2008). Identification, biochemical characterization, and subcellular localization of allantoate amidohydrolases from Arabidopsis and soybean. Plant Physiol. **146:** 418–430.

Werner, A.K., and Witte, C.P. (2011). The biochemistry of nitrogen mobilization: Purine ring catabolism. Trends Plant Sci. **16:** 381–387.

Witte, C.P., and Medina-Escobar, N. (2001). In-gel detection of urease with nitroblue tetrazolium and quantification of the enzyme from different crop plants using the indophenol reaction. Anal. Biochem. **290:** 102–107.

Witte, C.P., Noël, L.D., Gielbert, J., Parker, J.E., and Romeis, T. (2004). Rapid one-step protein purification from plant material using the eight-amino acid StrepII epitope. Plant Mol. Biol. **55:** 135–147.

Witte, C.P., Rosso, M.G., and Romeis, T. (2005). Identification of three urease accessory proteins that are required for urease activation in Arabidopsis. Plant Physiol. **139:** 1155–1162.

Wu, F.H., Shen, S.C., Lee, L.Y., Lee, S.H., Chan, M.T., and Lin, C.S. (2009). Tape-*Arabidopsis* Sandwich - A simpler *Arabidopsis* protoplast isolation method. Plant Methods **5:** 16.

Yuan, G., Bin, J.C., McKay, D.J., and Snyder, F.F. (1999). Cloning and characterization of human guanine deaminase. Purification and partial amino acid sequence of the mouse protein. J. Biol. Chem. **274:** 8175–8180.

Zrenner, R., Stitt, M., Sonnewald, U., and Boldt, R. (2006). Pyrimidine and purine biosynthesis and degradation in plants. Annu. Rev. Plant Biol. **57:** 805–836.